MedChemComm

Accepted Manuscript

Journal Name

ARTICLE

In silico-driven multicomponent synthesis of 4,5- and 1,5-disustituted imidazoles as indoleamine 2,3-dioxygenase inhibitors

Received 00th January 20xx,
Accepted 00th January 20xx

DOI: 10.1039/x0xx00000x

www.rsc.org/

S. Fallarini,[†] A. Massarotti,[†] A. Gesù, S. Giovarruscio, G. Coda Zabetta, R. Bergo, B. Giannelli, A. Brunco, G. Lombardi, G. Sorba and T. Pirali[*]

Indoleamine 2,3-dioxygenase is involved in pathological immune escape and has recently become an attractive target in anti-cancer therapy. 4-Phenylimidazole (4-PI) provides a promising starting point for the development of IDO1 inhibitors. With the aim of discovering more potent ligands, a virtual library of imidazoles synthesizable *via* the van Leusen multicomponent reaction was created and filtered to afford a set of 4,5- and 1,5-disubstituted imidazoles as virtual lead candidates. The compounds were selected according to their docking score and to their synthetic feasibility, synthesized and biologically evaluated. This experimental approach yielded IDO1 inhibitors with enhanced potency compared to 4-PI, the most active compounds displayed low micromolar potency, both in enzymatic and cellular assay, while showing no detectable cellular toxicity. A 3D quantitative structure-activity relationship based on the electrostatic and steric ligand-protein interactions was performed.

Introduction

The kynurenine pathway is the main route for the oxidative degradation of the amino acid tryptophan, and indoleamine 2,3-dioxygenase (IDO) catalyzes the first and rate-limiting step along this pathway.[1] Over the years, this enzyme has evolved conceptually from a simple tryptophan-catabolizing enzyme into an important player in tumor immune escape.[2] IDO1 inhibitors have recently been identified as a priority in translational research by the immune response modifier pathway prioritization working group from the NIH.[3] Indeed, several studies have offered evidences that IDO1 inhibition by small molecule inhibitors can exert anti-tumor effects, improving the efficacy of vaccination, chemotherapy or radiationtherapy.[4] As a possible drug development target, IDO1 has a number of appealing features. An *Ido1* gene knockout mouse has been reported to be viable and healthy,[5] indicating that IDO1 inhibitors will be unlikely to produce severe mechanism-based side-effects; tryptophan and kynurenine, the upstream substrate and downstream product of the IDO1-catalyzed reaction, may serve as biomarkers to monitor disease progression and response to therapy with IDO1 modulators; small-molecule inhibitors of IDO1 offer substantial cost advantages compared to biological or cell-based therapies that aim at modulating immune response; last, crystal structure of IDO1 has been solved[6] and this discovery has paved the way for computer-guided design and the synthesis of novel inhibitors. In this regard, the crystal structure of human IDO1 shows one binding pocket in the distal heme site (pocket A), connected to a second pocket towards the entrance of the active site (pocket B).

In 1989 4-phenylimidazole (4-PI, **1**, Fig. 1) was identified as a weak non-competitive inhibitor of IDO1[7] and in 2006 X-ray crystal structure of human IDO1 complexed with this ligand inhibitor was published,[6] showing that the imidazole is coordinated to the heme iron projecting its phenyl ring towards pocket A (Fig. 2). No other specific interactions with the enzyme were described, which explains the relative low potency of this inhibitor.

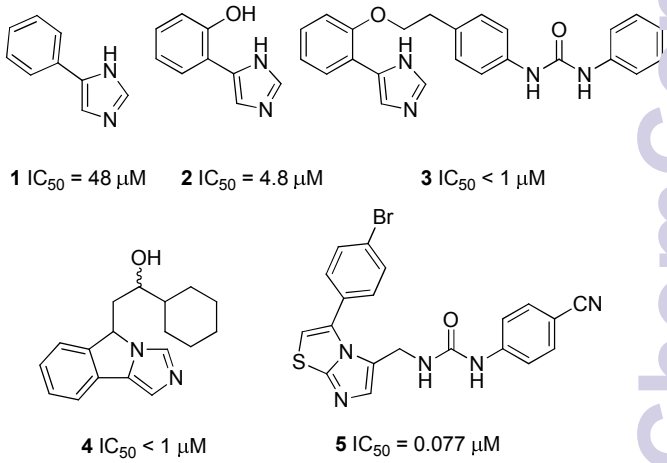

Fig. 1 Representative reported imidazoles as IDO1 inhibitors.

[a.] *Dipartimento di Scienze del Farmaco, Università degli Studi del Piemonte Orientale "A. Avogadro", Largo Donegani 2 28100 Novara, Italy.*
† These Authors contributed equally to this manuscript.
Electronic Supplementary Information (ESI) available. See DOI: 10.1039/x0xx00000x

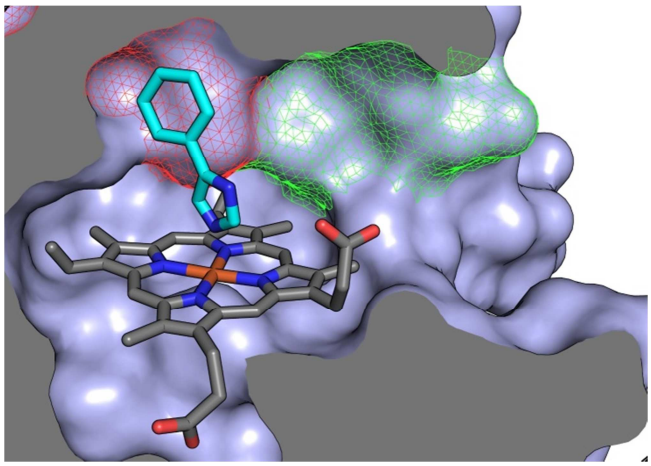

Fig. 2 Compound **1** bound to heme iron of IDO1. Heme depicted as grey sticks, compound **1** as cyan sticks. Red mesh: pocket A; green mesh: pocket B (PDB code: 2D0T).

In 2008, Newlink Genetics described the generation of 4-PI derivatives by introduction of substituents on the phenyl ring of **1**: interestingly, the introduction of a hydroxyl group in the 2'-position led to 10-fold higher potency at IDO1 inhibition compared with 4-PI, thanks to additional interactions with Ser167 in the interior of the IDO1 active site (**2**, Fig. 1).[8] Next year, the same company reported a large number of variously substituted 4-arylimidazoles together with a small set of 1,5-disubstituted imidazoles, showing at best IC_{50} values less than 20 μM.[9] Taking advantage of these results, in a 2011 application an extensive series of compounds displaying *O*-substituted 2'-hydroxyl-4-phenylimidazoles was described featuring a long extension into the B pocket, with an IDO1 inhibition in the nanomolar range (**3**, Fig. 1).[10] Finally, in 2012 a large number of fused phenyl-imidazoles was reported (**4**, Fig. 1),[11] leading to the identification of NLG919 (undisclosed structure, IC_{50} = 28 nM), an orally available IDO1 inhibitor that has recently entered Phase I clinical trials.[12] Recently, the X-ray structure of IDO1 bound to a novel imidazothiazole inhibitor (PDB id: 4PK6) became available, showing that both pockets A and B are occupied.[13] The most active compound described herein is **5** (Fig. 1), which displays a nanomolar potency thanks to the generation of an induced fit and the resulting interaction with Phe226 and Arg231. All these reported data point out the phenylimidazole scaffold as a promising starting point for the development of IDO1 inhibitors; indeed, its binding mode to the active site is known through X-ray crystallography, rational structural modifications of the imidazole ring have been shown to be feasible, and reasonable SAR studies are observed.

Driven by high atom and step economy, multicomponent reactions (MCRs) have emerged in the last 15 years as perfectly suited tools for the synthesis of collections of drug-like compounds to be used in hit to lead discovery.[14] In this context, our research team has successfully applied MCRs to the discovery of biologically active compounds.[15] In this work, we report the synthesis of 4-PI analogues *via* the van Leusen MCR, the most straightforward methodology to access to functionally rich imidazoles known to date.[16] This transformation can be exploited in the synthesis of four different series of compounds: 1,4,5-trisubstituted, 1,5- 1,4 and 4,5-disubstituted imidazoles (Scheme 1).

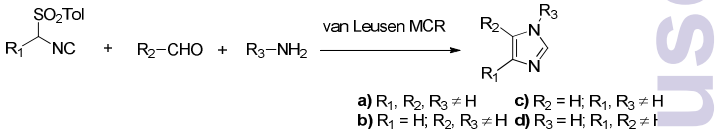

Scheme 1 The van Leusen multicomponent reaction.

The van Leusen reaction represents an efficient and mild protocol for preparing polysubstituted imidazoles in a single pot and in a completely regioselective manner from TosMIC reagents and imines generated *in situ* from an aldehyde and an amine. The utility of this transformation in medicinal chemistry is exemplified by the multi-kilogram scale synthesis of a potent and selective p38 kinase inhibitor that was promoted to Phase III clinical trials by Glaxo-Smith-Kline.[17] Due to the availability of many α-substituted TosMIC compounds, aldehydes and amines, the accessible imidazole chemical space is huge. However, it is neither practical nor possible to synthesize all interesting molecules and put them into a large compound repository. A promising and complementary strategy which leverages the strength of MCR chemistry and its exploratory power is the use of computational screening, and in particular of a structure-based virtual screening approach.

Results and Discussion

Virtual Screening

We have generated a virtual library of imidazoles synthesizable *via* the van Leusen MCR, developed a protocol for the structure-based virtual screening of these compounds towards IDO1, screened and filtered the virtual library, and identified a set of virtual lead candidates. The virtual library has been created using an *in house* enumerating script built in perl. As starting materials, we have collected all the aldehydes, amines and TosMIC compounds available from chemical vendors. The structures were downloaded using their web-based interface, considering 300 Daltons the upper limit for the molecular weight. Using these criteria, we retrieved about 1,000, 1,000 and 50 compounds for aldehydes, amines and TosMIC reagents, respectively. The theoretical chemical space of this virtual library was 50,000,000. The library was filtered for drug-like compounds and a conformer library was generated with the program OMEGA2.[18] The FRED software[19] was used in order to dock all the compounds in the IDO1 binding site and the simulated binding energy was used to rank them all. Last, an experienced medicinal chemist selected a set of virtual lead candidates according to their docking score and to their synthetic feasibility. The visual inspection of the ranked compounds revealed that all 1,4,5-trisubstituted and 1,4-disubstituted imidazoles were discarded, suggesting that their

substitution patterns suffer from steric hindrance compared to 1,5- and 4,5-disubstituted imidazoles and are not suitable for interaction with IDO1 binding site. 4,5-Disubstituted imidazoles display better docking poses and fifteen structures were selected (Table 1, **6**-**20**), while only ten 1,5-disubstituted imidazoles were considered (Table 1, **21**-**30**). Figure 3 depicts a docking pose of compound **15**, which shows one of the lowest score. 3-Bromophenyl ring is accommodated in the narrow and hydrophobic pocket A (Tyr126, Cys129, Val130, Phe163 and Phe164), while the more steric hindered *p*-acetamidophenyl substituent can fit in the extended pocket B (Phe226 and Arg231). The docked pose of the selected compounds shows that, while they all occupy both pockets A and B, the imidazole ring is oriented very differently relative to the heme group and is not always able to form a strong nitrogen-iron bond. A figure depicting all docking results of the synthesized compounds is available in the Supplementary Information.

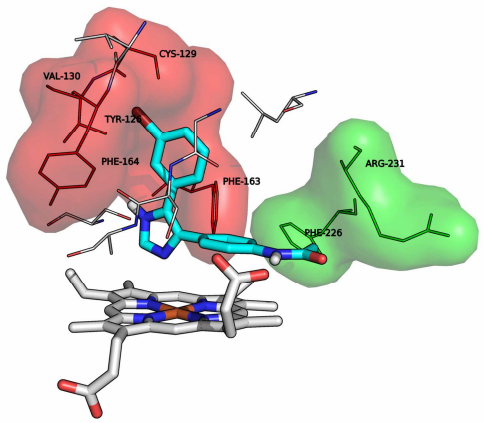

Fig. 3 Docked pose of compound **15** (cyan sticks). Pocket A is depicted as red lines, pocket B as green lines.

Chemistry

4,5-Disubstituted imidazoles were synthesized starting from α-substituted TosMIC derivatives **h-n**. Interestingly, even these precursors were prepared by a three-component reaction, where *p*-toluensulphinic acid, aldehyde and formamide reacted in the presence of TMSiCl in toluene and acetonitrile to yield formamides **a-g** (see Supplementary Information). Subsequent dehydration performed with phosphorous oxychloride and triethylamine in THF gave access to the α-functionalized TosMIC derivatives **h-n**, stable crystalline and easily-handled compounds (Scheme 2) (see Supplementary Information).[20]

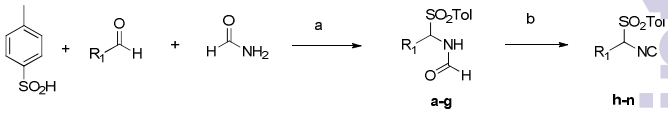

Scheme 2 Preparation of α-substituted TosMIC derivatives. Reagents and conditions: (a) TMSiCl, acetonitrile, toluene, 50 °C; (b) $POCl_3$, TEA, THF, -10 °C.

4,5-Disubstituted imidazoles (**6**-**20**, Table 1) were synthesized replacing primary amines with aqueous ammonium hydroxide (Scheme 3).[21]

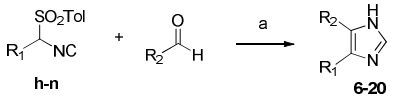

Scheme 3 Synthesis of 4,5-disubstituted imidazoles. Reagents and conditions: (a) Piperazine, NH_4OH aq. 30%, THF, rt.

Different functionalities could be accommodated in this mild basic process (acetamido, hydroxyl, halogen, methoxy, trifluoromethoxy groups). The reaction provided the desired imidazoles in moderate (**7**, **10**, **13**, **15**, **17**, **19**, **20**) to excellent (**6**, **11**, **12**, **16**) yields, while in some cases the yields were poor (**8**, **9**, **14**, **18**). The transformation worked with both aryl- and heteroaryl- (**20**) substituted TosMIC reagents. While *o*-fluorophenylsubstituted TosMIC derivatives underwent clean cycloaddition to form the corresponding imidazoles (**10**-**12**), *o*-methoxy- and *o*-chlorophenylsubstituted TosMIC reagents gave lower yields (**13**, **14**, **18**), which can be attributed to the increased congestion surrounding the benzylic carbon. Regarding the carbonyl counterpart, both aryl and benzyl (**14**) aldehydes were used, while electron-poor aldehydes (**8**, **9**) reacted sluggishly.

1,5-Disubstituted imidazoles (**21**-**30**, Table 1) were synthesized using TosMIC itself, aryl aldehydes and primary aliphatic amines in the presence of dimethylformamide as solvent and potassium carbonate as mild base (Scheme 4). The reaction was compatible with different functional groups (halogen, hydroxyl, secondary amine, acetamido, methoxy moieties) leading to the desired imidazoles in moderate yields under protecting group-free conditions.

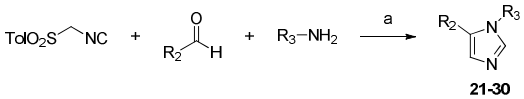

Scheme 4 Synthesis of 1,5-disubstituted imidazoles. Reagents and conditions: (a) K_2CO_3, DMF, rt.

Biological Evaluation and Structure-Activity Relationships (SAR) Findings

Cytotoxicity. The measurement of cell viability is mandatory when reporting cellular IDO1 inhibitory activity, because the observed reduction of tryptophan degradation could simply be an effect of cytotoxicity. Thus, we decided to first investigate the cytotoxicity of all the synthesized compounds on A375 cell line. Cells were treated (48 h) with increasing concentrations

(0.01-100 μM) of each compound and cell viability was measured by MTT assay. As shown in Table 1, the compounds **24**-**26**, **29** and **30** affected cell viability at the highest concentration tested (100 μM), while the other compounds resulted non-cytotoxic and biocompatible at all concentrations tested. These results prompted us to subject each compound to further biological evaluation and to use them up to 30 μM, a non-cytotoxic concentration for all compounds in this cell line.

Cellular IDO1 inhibitory activity. The ability of each compound to inhibit human IDO1 activity was first determined in an *in vitro* cell-based assay, which evaluates not only the inhibitory effect of the compounds, but also their capacity to permeate the cell membrane. IDO1 expression was induced in A375 cells by IFN-γ (500 U/mL) treatment (48 h) and enzymatic activity was determined by measuring the formation of the L-kynurenine (L-KYN) product by high-performance liquid chromatography (HPLC) method. IFN-γ treatment induced the expression of functional IDO1 in A375 cell line, consequently resulting in L-KYN release in the cell culture supernatant (data not shown). The ability of increasing concentrations (0.01–30 μM) of each compound to inhibit IFN-γ-mediated L-KYN production was therefore determined. Results are shown in Table 1 (see Supplementary Information for cellular concentration-response curves).

Compounds **6**-**11**, **15**-**18**, **20** and **21** resulted active as IDO1 inhibitors; in detail, compounds **6**, **8**-**11**, **15**-**16**, **20** and **21** showed IC_{50} values less than 5 μM, while compounds **7**, **17** and **18** showed IC_{50} values greater than 5 μM. The most potent IDO1 inhibitor was compound **8** with an IC_{50} of 1.5 μM. No inhibition was observed for compounds **12**-**14**, **19** and **21**-**30** up to the highest tested concentration of 30 μM. Surprisingly, **1**, that is reported to display a good inhibitory activity in enzymatic assay,[8] did not exhibit inhibitory activity on IDO1 in cellular assay at any tested concentration. These data has shown the predictively limitation of our virtual screening protocol considering that several top ranked compounds have not IDO1 inhibitory capability.

Regarding 4,5-disubstituted imidazoles, all substitutions in *ortho* position of the phenyl ring reduce the IDO1 inhibitory activity (**10**-**14**, **18**, **19**). Substitutions in *meta* positions are tolerated (**6**-**9**, **15**-**17**) and the presence of halogens yields better IDO1 inhibitors (**8**, **9**, **15**, **17**). Substituents in *para* position are compatible with the binding pocket (acetamido, methoxy, hydroxyl, trifluoromethoxy groups), leading to a wide variability of IC_{50} values, ranging from 2.9 μM (**15**) to no detectable activity (**12**, **13**, **19**) according to the substitution pattern of the other phenyl ring. 1,5-Disubstituted imidazoles are inactive, with the only exceptions of **21**.

Table 1 Cytotoxicity and cellular IDO1 inhibition activity of **1** and the synthesized compounds.

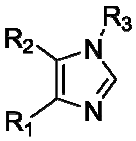

Cpd	Yield (%)	R_1	R_2	R_3	Cell viability (%) at 100 μM ± S.E.M.	IC_{50} (μM)
1	-	Phenyl	H	H	100 ± 5.1	>30
6	84	Phenyl	4-Hydroxy-3-methoxyphenyl	H	97 ± 5.6	3.5 ± 0.6
7	53	Phenyl	3,4-Dihydroxyphenyl	H	100 ± 8.4	6.3 ± 1.2
8	35	Phenyl	3-Bromophenyl	H	96 ± 8.6	1.5 ± 0.1
9	32	Phenyl	3-Chlorophenyl	H	97 ± 10.5	1.7 ± 0.1
10	54	2-Fluorophenyl	4-Acetamidophenyl	H	100 ± 2.5	4.7 ± 0.8
11	98	2-Fluorophenyl	3-Hydroxy-4-methoxyphenyl	H	100 ± 4.3	4.9 ± 1.1
12	80	2-Fluorophenyl	4-Hydroxyphenyl	H	98 ± 3.6	>30
13	58	2-Chlorophenyl	4-Methoxyphenyl	H	100 ± 8.6	>30
14	19	2-Chlorophenyl	Benzyl	H	98 ± 10.4	>30
15	44	3-Bromophenyl	4-Acetamidophenyl	H	100 ± 9.8	2.9 ± 0.5
16	95	3-Methylphenyl	4-Hydroxy-3-methoxyphenyl	H	98 ± 9.5	3.8 ± 1.2
17	64	3-Methylphenyl	3-Bromo-4-Hydroxyphenyl	H	100 ± 7.2	5.4 ± 1.1
18	32	2-Methoxyphenyl	3-Hydroxy-4-methoxyphenyl	H	99 ± 7.4	7.2 ± 1.2
19	48	2-Methylphenyl	3-Hydroxy-4-methoxyphenyl	H	100 ± 3.2	>30
20	40	Thiophen-3-yl	4-Trifluoromethoxyphenyl	H	98 ± 6.8	2.1 ± 0.8
21	49	H	5-Bromo-2-hydroxyphenyl	2-(Naphthalen-1-ylamino)ethyl	98 ± 10.3	3.4 ± 0.9
22	35	H	4-Methoxynaphthalen-1-yl	2-(Naphthalen-1-ylamino)ethyl	97 ± 7.2	>30
23	44	H	4-Phenoxyphenyl	2-(Naphthalen-1-ylamino)ethyl	100 ± 10.2	>30
24	30	H	4-Bromophenoxy)phenyl	2-(Naphthalen-1-ylamino)ethyl	22 ± 4.2	>30
25	35	H	2,6-Difluoro-3-hydroxyphenyl	2-(Naphthalen-1-ylamino)ethyl	53 ± 9.8	>30
26	47	H	3,5-Dibromo-2-hydroxyphenyl	2-(Naphthalen-1-ylamino)ethyl	39 ± 8.9	>30
27	55	H	2-Chloro-4-hydroxyphenyl	2-(Naphthalen-1-ylamino)ethyl	99 ± 1.5	>30
28	36	H	2-Hydroxy-5-methoxyphenyl	Cyclopropyl	96 ± 3.7	>30
29	26	H	4-Phenoxyphenyl	2-Acetamidoethyl	87 ± 6.8	>30
30	50	H	2-Hydroxy-5-methoxyphenyl	Propyl	89 ± 2.3	>30

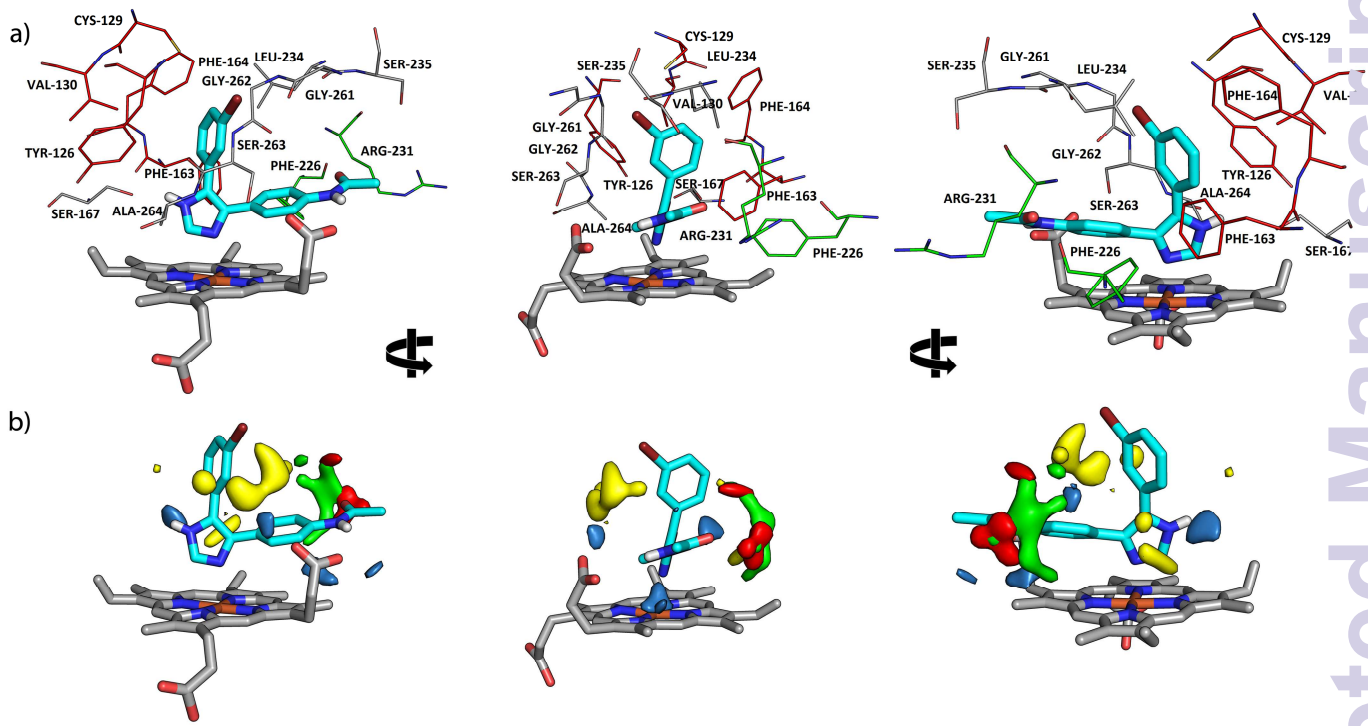

Fig. 4 (a) Different views of IDO1 active site (PDB id: 2D0T). Depicted compound: **15**, as cyan sticks. Red lines: pocket A, green lines: pocket B. (b) Different views of interaction fields derived from the 3D-QSAR analysis. Depicted compound: **15** (cyan sticks). Electrostatic effects: favourable (blue) and unfavourable (red). Steric effects: favourable (green) and unfavourable (yellow). Iron-nitrogen distance for the heme-bound nitrogen: 2.4 Å.

Enzymatic IDO1 inhibition. To evaluate whether the inhibitory activity of tested compounds could be influenced by their ability to permeate cell membranes, **1** and the most potent compounds (IC_{50} < 3 μM) were also tested in an enzymatic assay. Compounds **8**, **9**, **15** and **20** resulted active as IDO1 inhibitors showing an IC_{50} comparable with that obtained in the cellular assay (see Supplementary Information for enzymatic concentration-response curves and computed Hill slope values). In enzymatic assay 4-PI inhibited IDO1 activity with a potency similar to that reported by Kumar and colleagues,[8] confirming that **1** is active as IDO1 inhibitor. These results also suggest that the data obtained in the cellular assay could be due to an intrinsic inability of 4-PI in crossing the cell membrane.

Table 2 Enzymatic IDO1 inhibition activity of **1** and compounds **8**, **9**, **15**, **20**.

Cpd	Enzymatic IC_{50} (μM)
1	48.0 ± 4.5
8	1.9 ± 0.6
9	4.7 ± 1.1
15	2.8 ± 0.5
20	4.5 ± 1.2

3D-Quantitative Structure-Activity Relationship (QSAR) Analysis.

As a strong correlation between docking scores and biological activity was not found, a different approach was used to analyze the experimental data. Exploiting the results obtained in the cellular IDO1 inhibitory assay, we attempted to find a consistent relationship between biological activity and 3D structures of the synthesized 4,5-disubstituted imidazoles. As the 1,5-disubstituted compounds displayed poor inhibition activity together with a narrow range of pIC_{50}, they were not included in our study. The molecules were aligned using Open3DAlign, which generates one structure-and-field based alignment of the data set using each compound as a template. During visual inspection, the best alignment was selected to perform the analysis, according to alignment scores and superposition of imidazole substituents. Open3DQSAR[22] and Forge[23] software were used, with the aim to provide the regions in space where interactive fields may influence the activity. The 3D-QSAR models were derived for a data set of 15 compounds using 75% of the compounds in the training set and 25% in the test set. The compounds of both training and test sets were carefully selected in order to cover the entire range of activity values. The model was evaluated by measuring its accuracy in predicting the activity using Forge software.[23] The results confirmed the reliability of the 3D-QSAR model, considering the statistical values obtained for the left-one-out (LOO) analyses (R^2 = 0.998, Q^2 = 0.555). We manually placed the 3D-QSAR model and its Molecular Interaction Fields (MIFs) inside IDO1 active site according to

the pockets shapes and the surrounding aminoacids using PyMOL software.[24] In Figure 4 MIFs and compound **15** are shown. It is possible to appreciate favorable steric contribution (green) to the predicted activity nearby the acetamido group, that protrudes into the almost unoccupied pocket B, and unfavorable steric effects (yellow) surrounding the bromophenyl substituent, that is placed in the narrow and hydrophobic pocket A. Interestingly, compound **15** displays good electrostatic interactions (blue) at the rear of pocket A; this field points to Ser167, suggesting that a hydrogen bond between the NH of the imidazole ring and this residue of the protein can be formed. This interaction is peculiar of our 4,5-disubstituted imidazoles. Indeed, 4-substituted imidazoles are not prone to form this hydrogen-bond, as demonstrated by the X-ray crystal structure of IDO1 complexed with **1**.[6] Further exploration of this interaction near pocket A might improve the activity of 4,5-disubstituted imidazoles, while in pocket B electrostatic interactions are found to have a negative effect (red) and should be carefully considered in the next generation of compounds.

Experimental

Chemistry

Materials and Instrumentation. 1 and commercially available reagents and solvents were purchased from Sigma-Aldrich and Alfa Aesar and used without further purification. When needed, the reactions were performed in flame- or oven-dried glassware under a positive pressure of dry N_2. Melting points were determined in open glass capillary with a Stuart scientific SMP3 apparatus. All the target compounds were checked by IR (FT-IR Thermo-Nicolet Avatar), ^{1}H and ^{13}C APT (Jeol ECP 300 MHz), and mass spectrometry (Thermo Finningan LCQ-deca XP-plus) equipped with an ESI source and an ion trap detector. Chemical shifts are reported in parts per million (ppm). Column chromatography was performed on silica gel Merck Kieselgel 70-230 mesh ASTM. Thin layer chromatography (TLC) was carried out on 5 cm × 20 cm plates with a layer thickness of 0.25 mm (Merck silica gel 60 F254). When necessary, they were visualized with $KMnO_4$. The purity of the target compounds (> 95%) was determined via elemental analysis and was within ± 0.4% of the calculated value.

General procedure for the synthesis of 4,5-disubstituted imidazoles. To a solution of aldehyde (1.5 equiv) in THF an ammonium hydroxide (4 equiv) solution (30% in water) is added. After stirring for one hour at room temperature, tosylmethylisocyanide (1 equiv) and piperazine (1.5 equiv) are added. The reaction is stirred overnight at room temperature. The solvent is evaporated and the crude material is purified by column chromatography.

2-Methoxy-4-(5-phenyl-1H-imidazol-4-yl)phenol (6). Brown solid. Yield: 84%. mp 113-114 °C. Found: C, 72.34; H, 5.35; N, 10.71. $C_{16}H_{14}N_2O_2$ requires C, 72.16; H, 5.30; N, 10.52. ν_{max}/cm^{-1} 3064, 2814, 2345, 1731, 1519, 1260, 1215, 1125, 769, 698. ^{1}H NMR δ_H (300 MHz; DMSO-d$_6$) 7.75 (s, 1 H), 7.53 (d, *J* = 6.8 Hz, 2 H), 7.32 (t, *J* = 6.8 Hz, 2 H), 7.21 (m, 1 H), 7.03 (s, 1 H), 6.89 (d, *J* = 7.9 Hz, 1 H), 6.78 (d, *J* = 7.9 Hz, 1 H), 3.66 (s, 3 H). ^{13}C NMR δ_C (75 MHz; DMSO-d$_6$) 172.7, 170.9, 147.9, 146.5, 135.5, 134.6, 128.7, 127.8, 127.1, 124.5, 120.9, 116.1, 112.5, 55.9. m/z 267 (M$^+$).

4-(5-Phenyl-1H-imidazol-4-yl)benzene-1,2-diol (7). Light brown solid. Yield: 53%. mp 81-82 °C. Found: C, 71.48; H, 4.83; N, 11.05. $C_{15}H_{12}N_2O_2$ requires C, 71.42; H, 4.79; N, 11.10. ν_{max}/cm^{-1} 3129, 3060, 2295, 1874, 1514, 1274, 1116, 769, 697. ^{1}H NMR δ_H (300 MHz; CD$_3$OD) 7.75 (s, 1 H), 7.45 (d, *J* = 7.9 Hz, 2 H), 7.29-7.17 (m, 3 H), 6.88 (s, 1 H), 6.77-6.75 (m, 2 H) . ^{13}C NMR δ_C (75 MHz; CD$_3$OD) 145.1 (2 C), 132.9, 131.2, 131.0, 128.9, 128.2, 127.5, 126.9, 125.5, 123.7, 119.8, 115.2. m/z 253 (M$^+$).

4-(3-Bromophenyl)-5-phenyl-1H-imidazole (8). White solid. Yield: 35%. mp 178-179 °C. Found: C, 60.30; H, 3.80; N, 9.45. $C_{15}H_{11}BrN_2$ requires C, 60.22; H, 3.71; N, 9.36. ν_{max}/cm^{-1} 2816, 2642, 1598, 1481, 958, 769. ^{1}H NMR δ_H (300 MHz; DMSO-d$_6$) 7.81 (s, 1 H), 7.[illegible] (m, 1 H), 7.49-7.20 (m, 7H), 7.22 (m, 1 H). ^{13}C NMR δ_C (75 MHz; DMSO-d$_6$) 137.0, 136.6, 131.0 (2C), 130.0, 129.9 (2 C), 129.2, 128.4 (2C), 128.1, 126.4, 122.2. m/z 300 (M$^+$).

4-(3-Chlorophenyl)-5-phenyl-1H-imidazole (9). White solid. Yield: 32%. mp 175-176 °C. Found: C, 70.78; H, 4.40; N, 11.12. $C_{15}H_{11}ClN_2$ requires C, 70.73; H, 4.35; N, 11.00. ν_{max}/cm^{-1} 3055, 2985, 1600, 1509, 1470, 1273, 971, 767, 699, 652. ^{1}H NMR δ_H (300 MHz; DMSO-d$_6$) 7.80 (s, 1 H), 7.51-7.26 (m, 9 H). ^{13}C NMR δ_C (75 MHz; DMSO-d$_6$) 136.6, 133.7, 132.5, 130.8, 129.2, 129.0, 128.4, 128.1, 128.0, 127.5, 127.2, 127.0, 126.1. m/z 255 (M$^+$)

***N*-(4-(5-(2-Fluorophenyl)-1H-imidazol-4-yl)phenyl)acetamide (10)**. Yellow solid. Yield: 54%. mp 214-215 °C. Found: C, 69.28; H, 4.76; N, 14.24. $C_{17}H_{14}FN_3O$ requires C, 69.14; H, 4.78; N, 14.23. ν_{max}/cm^{-1} 3450, 2382, 2152, 1583, 1151, 955, 577, 412. ^{1}H NMR δ_H (300 MHz; CD$_3$OD) 7.80 (s, 1 H), 7.48 (d, *J* = 8.5 Hz, 2 H), 7.42-7.33 (m, 2 H), 7.30 (d, *J* = 8.5 Hz, 2 H), 7.23-7.12 (m, 2 H), 2.10 (s, 3 H). ^{13}C NMR δ_C (75 MHz; DMSO-d$_6$) 168.9, 159.6 (d, *J* = 245.0 Hz), 138.7, 136.[illegible] 132.3, 131.0 (2 C), 130.9, 129.5, 126.9, 125.2, 119.9, 119.5, 116.6, 24.4. m/z 296 (M$^+$)

5-(5-(2-Fluorophenyl)-1H-imidazol-4-yl)-2-methoxyphenol (11). Yellow solid. Yield: 98%. mp 109-110 °C. Found: C, 67.65; H, 4.71; N, 9.91. $C_{16}H_{13}FN_2O_2$ requires C, 67.60; H, 4.61; N, 9.85. ν_{max}/cm^{-1} 3528, 3002, 2838, 1590, 1515, 1254, 1216, 1129, 884, 816, 761. ^{1}H NMR δ_H (300 MHz; DMSO-d$_6$) 8.90 (br s, 1 H), 7.75 (s, 1 H), 7.46-7.38 (m, 2 H), 7.25-7.21 (m, 2 H), 6.84-6.72 (m, 3 H), 3.73 (s, 3 H). ^{13}C NMR δ_C (75 MHz; DMSO-d$_6$) 159.9 (d, *J* = 245.0 Hz), 147.4, 147.2 (d, *J* = 38.4 Hz), 146.7, 138.2, 136.0, 132.4, 130.0, 125.0, 117.8, 116.3 (d, *J* = 21.1 Hz), 114.4 (2 C), 112.6 (2 C), 56.0. m/z 285 (M$^+$)

4-(5-(2-Fluorophenyl)-1H-imidazol-4-yl)phenol (12). Yellow solid. Yield: 80%. mp 99-100 °C. Found: C, 70.90; H, 4.35; N, 11.12. $C_{15}H_{11}FN_2O$ requires C, 70.86; H, 4.36; N, 11.02. ν_{max}/cm^{-1} 3637, 3057, 2666, 2289, 1612, 1516, 1451, 1263, 1171, 836, 760. ^{1}H NMR δ_H (300 MHz; CD$_3$OD) 7.75 (s, 1H), 7.36-7.29 (m, 2H), 7.19 (d, *J* = 8.5 Hz, 2H), 7.14-7.09 (m, 2H), 6.72 (d, *J* = 8.5 Hz, 2H). ^{13}C NMR δ_C (75 MHz; CD$_3$OD) 160.0 (d, *J* = 245.6 Hz), 156.7, 133.0, 131.5, 129.4 (d, *J* = 8.0 Hz), 128.1, 125.1, 124.0 (d, *J* = 3.4 Hz), 123.5, 121.3 (d, *J* = 14.[illegible] Hz), 115.7 (d, *J* = 21.7 Hz), 115.0 (2C). m/z 255 (M$^+$)

5-(2-Chlorophenyl)-4-(4-methoxyphenyl)-1H-imidazole (13). White solid. Yield: 58%. mp 239-240 °C. Found: C, 67.59; H, 4.65; N, 9.88. $C_{16}H_{13}ClN_2O$ requires C, 67.49; H, 4.60; N, 9.84. ν_{max}/cm^{-1} 2835, 1616, 1470, 1246, 1178, 834, 762. ^{1}H NMR δ_H (300 MHz; CD$_3$OD) 7.75 (s, 1 H), 7.48 (d, *J* = 7.1 Hz, 1 H), 7.39-7.30 (m, 3 H), 7.20 (d, *J* =

8.5 Hz, 2 H), 6.80 (d, *J* = 8.5 Hz, 2 H), 3.75 (s, 3 H). ^{13}C NMR δ_C (75 MHz; DMSO-d$_6$) 158.5, 146.1, 135.8, 135.7, 133.9, 133.4, 133.3, 130.4, 130.2, 127.8, 127.5, 127.4, 114.3, 55.6. m/z 285 (M$^+$)

4-Benzyl-5-(2-chlorophenyl)-1H-imidazole (14). Yellow solid. Yield: 19%. mp 166-167 °C (dec). Found: C, 71.69; H, 4.96; N, 10.45. $C_{16}H_{13}ClN_2$ requires C, 71.51; H, 4.88; N, 10.42. ν_{max}/cm^{-1} 2632, 1483, 1430, 1255, 1061, 966, 758. ^{1}H NMR δ_H (300 MHz; DMSO-d$_6$) 7.85 (s, 1 H), 7.50 (m, 1 H), 7.34-7.15 (m, 8 H), 3.09 (s, 2 H). ^{13}C NMR δ_C (75 MHz; DMSO-d$_6$) 140.3, 139.9, 136.2, 132.9, 132.5, 130.2, 129.8, 129.7, 129.1, 128.9, 128.8, 127.5, 124.2, 48.0. m/z 270 (M$^+$)

***N*-(4-(5-(3-Bromophenyl)-1H-imidazol-4-yl)phenyl)acetamide (15)**. Yellow solid. Yield: 44%. mp 234-235 °C (dec). Found: C, 57.40; H, 3.96; N, 11.85. $C_{17}H_{14}BrN_3O$ requires C, 57.32; H, 3.96; N, 11.80. ν_{max}/cm^{-1} 2360, 2057, 1650, 1463, 1401, 984, 841, 686. ^{1}H NMR δ_H (300 MHz; CD$_3$OD) 7.76 (s, 1 H), 7.63 (s, 1 H), 7.56 (d, *J* = 7.7 Hz, 2 H), 7.40-7.34 (m, 4 H), 7.20 (t, *J* = 7.9 Hz, 1 H), 2.13 (s, 3 H). ^{13}C NMR δ_C (75 MHz; DMSO-d$_6$) 169.1, 139.6, 138.4, 136.2, 134.4, 130.9, 129.6, 129.3, 129.2, 128.3, 125.9, 122.2,119.6,119.4, 24.6. m/z 358 (M$^+$)

2-Methoxy-4-(5-(*m*-tolyl)-1H-imidazol-4-yl)phenol (16) . White solid. Yield: 95%. mp 145-146 °C. Found: C, 72.90; H, 5.79; N, 9.99. $C_{17}H_{16}N_2O_2$ requires C, 72.84; H, 5.75; N, 9.99. ν_{max}/cm^{-1} 3508, 2831, 1733, 1599, 1463, 1261, 1214, 1123, 1034, 788. ^{1}H NMR δ_H (300 MHz; CDCl$_3$) 7.62 (s, 1 H), 7.36 (s, 1 H), 7.28 (d, *J* = 7.4 Hz, 1 H), 7.19 (t, *J* = 7.4 Hz, 1 H), 7.09-7.06 (m, 2 H), 6.98 (d, *J* = 8.2 Hz, 1 H), 6,83 (d, *J* = 8.2 Hz, 1 H), 3.73 (s, 3 H), 2.30 (s, 3 H). ^{13}C NMR δ_C (75 MHz; DMSO-d$_6$) 153.7, 148.8, 147.9, 146.4, 142.6, 138.1, 135.5, 134.3, 128.7, 128.5, 127.8, 125.1, 120.8, 116.0, 112.4, 55.9, 21.6. m/z 281 (M$^+$)

2-Bromo-4-(5-(*m*-tolyl)-1H-imidazol-4-yl)phenol (17). White solid. Yield: 64%. mp 213-214 °C. Found: C, 58,43; H, 4.00; N, 8.55. $C_{16}H_{13}BrN_2O$ requires C, 58.38; H, 3.98; N, 8.51. ν_{max}/cm^{-1} 3399, 3145, 1573, 1507, 1428, 1286, 1156, 828, 624. ^{1}H NMR δ_H (300 MHz; DMSO-d$_6$) 7.79 (s, 1 H), 7.58 (s, 1 H), 7.32 (s, 1 H), 7.25-7.21 (m, 3 H), 7.08 (m, 1H), 6.91(d, *J* = 8.2 Hz, 1 H), 2.28 (s, 3 H). ^{13}C NMR δ_C (75 MHz; DMSO-d$_6$) 153.8, 138.1, 135.8, 133.2, 132.3, 130.8, 130.7, 128.9, 128.6, 128.4, 128.3, 126.3, 125.2, 116.8, 109.8, 21.6 . m/z 329 (M$^+$)

2-Methoxy-5-(5-(2-methoxyphenyl)-1H-imidazol-4-yl)phenol (18). Yellow solid. Yield: 32%. mp 208-209 °C. Found: C, 68.99; H, 5.46; N, 9.55. $C_{17}H_{16}N_2O_3$ requires C, 68.91; H, 5.44; N, 9.45. ν_{max}/cm^{-1} 3009, 2932, 1513, 1483, 1287, 1244, 1023, 752. ^{1}H NMR δ_H (300 MHz; CD$_3$OD) 7.70 (s, 1 H), 7.30 (t, *J* = 8.2 Hz, 1 H), 7.22 (d, *J* = 7.4 Hz, 1 H), 7.02 (d, *J* = 7.4 Hz, 1 H), 6.96-6.78 (m, 4 H), 3.80 (s, 3 H), 3.67 (s, 3 H). ^{13}C NMR δ_C (75 MHz; DMSO-d$_6$) 157.5, 156.5, 146.7, 146.4, 135.1, 131.9, 129.9, 128.8, 120.9, 120.5, 117.7, 114.4, 112.4, 112.2, 111.7. m/z 297 (M$^+$)

2-Methoxy-5-(5-(*o*-tolyl)-1H-imidazol-4-yl)phenol (19). Yellow solid. Yield: 48%. mp 204-205 °C. Found: C, 72.90; H, 5.79; N, 9.99. $C_{17}H_{16}N_2O_2$ requires C, 72.84; H, 5.75; N, 9.99. ν_{max}/cm^{-1} 3550, 3359, 2931, 2495, 2238, 1928, 1440, 1268, 1126, 772. ^{1}H NMR δ_H (300 MHz; DMSO-d$_6$) 8.81 (s, 1 H), 7.69 (s, 1 H), 7.42-7.13 (m, 4 H), 6.88 (s, 1 H), 6.75 (d, *J* = 8.2 Hz, 1 H), 6.65 (d, *J* = 8.2 Hz, 1 H), 3.70 (s, 3 H), 2.04 (s, 3 H). ^{13}C NMR δ_C (75 MHz; DMSO-d$_6$) 153.9, 147.5, 146.8, 146.7, 137.5 (2 C), 131.2, 130.7, 130.4, 128.5, 126.3, 124.9, 117.2, 114.0, 112.6, 56.2, 20.2. m/z 281 (M$^+$)

5-(Thiophen-3-yl)-4-(4-(trifluoromethoxy)phenyl)-1H-imidazole (20). Light pink solid. Yield: 40%. mp 180-181 °C. Found: C, 54.28; H, 3.00; N, 9.13. $C_{14}H_9F_3N_2OS$ requires C, 54.19; H, 2.92; N, 9.03. ν_{max}/cm^{-1} 2830, 1509, 1460, 1258, 837, 768, 653, 547. ^{1}H NMR δ_H (300 MHz; DMSO-d$_6$) 7.78 (s, 1 H), 7.68-7.55 (m, 3 H), 7.33 (m, 1 H), 7.12 (d, *J* = 5.0 Hz, 1 H). ^{13}C NMR δ_C (75 MHz; DMSO-d$_6$) 147.6, 144.5, 136.2, 134.5, 129.4, 127.9, 127.7, 127.2, 126.5, 122.9, 121.5, 120.7 (q, *J* = 254.2 Hz, 1 H). m/z 311 (M$^+$)

General procedure for the synthesis of 1,5-disubstituted imidazoles. To a solution of aldehyde (1 equiv) in dry DMF, amine (1 equiv) is added. The reaction is stirred at room temperature under a nitrogen atmosphere for one hour. K_2CO_3 (3 equiv) and TosMIC (1.5 equiv) are added. When the reaction is complete (typically after 24 hours), the reaction is diluted with EtOAc and washed with water (x 1). The organic layer is dried over sodium sulfate and evaporated. The crude material is purified by column chromatography.

4-Bromo-2-(1-(2-(naphthalen-1-ylamino)ethyl)-1H-imidazol-5-yl)phenol (21). Light green solid. Yield: 49%. mp 190-191 °C (dec). Found: C, 61,85; H, 4.49; N, 10.33. $C_{21}H_{18}BrN_3O$ requires C, 61.78; H, 4.44; N, 10.29. ν_{max}/cm^{-1} 2852, 1731, 1581, 1494, 1411, 1278, 1110, 771. ^{1}H NMR δ_H (300 MHz; CD$_3$OD) 7.81 (m, 1 H), 7.71-7.68 (m, 2 H), 7.37-7.34 (m, 3 H), 7.25 (m, 1 H), 7.14-7.18 (m, 2 H), 6.90 (s, 1 H), 6.81 (d, *J* = 8.8 Hz, 1 H), 6.23 (d, *J* = 7.1 Hz, 1 H), 4.26 (q, *J* = 6.3 Hz, 2 H), 3.64 (t, *J* = 6.3 Hz, 1 H), 3.50 (t, *J* = 6.3 Hz, 2 H). ^{13}C NMR δ_C (75 MHz; CDCl$_3$) 155.0, 142.4, 139.9, 139.8, 139.7, 139.6, 134.0, 133.3, 133.2, 132.7, 128.6, 128.5, 126.8, 126.2, 125.5, 123.4, 117.7, 111.0, 103.5, 60.3, 43.9. m/z 409 (M$^+$)

***N*-(2-(5-(4-methoxynaphthalen-1-yl)-1H-imidazol-1-yl)ethyl)naphthalen-1-amine (22)**. Brown oil. Yield: 35%. Found: C, 79.41; H, 5.95; N, 10.68. $C_{26}H_{23}N_3O$ requires C, 79.36; H, 5.89; N, 10.68. ν_{max}/cm^{-1} 3341, 2935, 1838, 1671, 1586, 1080, 765. ^{1}H NMR δ_H (300 MHz; CDCl$_3$) 8.35 (d, *J* = 8.0 Hz, 1 H), 7.75-7-72 (m, 2 H), 7.56-7.33 (m, 7 H), 7.15-7.07 (m, 2 H), 7.15 (t, *J* = 8.0 Hz, 1 H), 6.79 (d, *J* = 8.0 Hz, 1 H), 5.98 (d, *J* = 8.0 Hz, 1 H), 4.07-4.03 (m, 5 H), 3.34 (t, *J* = 5.8 Hz, 2 H), 2.27 (br s, 1 H). ^{13}C NMR δ_C (75 MHz; DMSO-d$_6$) 156.1, 143.5, 138.8, 134.5, 134.0, 131.6, 130.6, 130.4, 129.0, 128.4, 127.9, 126.9, 126.1, 125.5, 125.4, 124.5, 123.5, 122.5, 122.0, 119.5, 116.2, 104.5, 103.0, 60.3, 44.5, 44.3. m/z 394 (M$^+$)

***N*-(2-(5-(4-phenoxyphenyl)-1H-imidazol-1-yl)ethyl)naphthalen-1-amine (23)**. Brown oil. Yield: 44%. Found: C, 79.95; H, 5.70; N, 10.35. $C_{27}H_{23}N_3O$ requires C, 79.97; H, 5.72; N, 10.36. ν_{max}/cm^{-1} 3050, 1903, 1582, 1482, 1237, 770. ^{1}H NMR δ_H (300 MHz; CDCl$_3$) 7.76 (d, *J* = 7.9 Hz, 1 H), 7-63-7.58 (m, 2 H), 7.47-7.35 (m, 8 H), 7.16 (t, *J* = 7.1 Hz, 1 H), 7.07-7.04 (m, 3 H), (6.99 (d, *J* = 7.7 Hz, 2 H), 6.37 (m, 1 H), 4.31 (t, *J* = 6.0 Hz, 2 H), 3.55-3.53 (m, 2 H). ^{13}C NMR δ_C (75 MHz; DMSO-d$_6$) 157.2, 156.7, 143.7, 139.4, 134.6, 132.4, 130.9, 130.7, 128.5, 127.9, 127.2, 126.2, 125.3, 124.6, 124.4, 123.6, 122.0, 119.7, 119.0, 116.5, 103.5, 44.3, 43.7. m/z 406 (M$^+$)

***N*-(2-(5-(4-(4-bromophenoxy)phenyl)-1H-imidazol-1-yl)ethyl)naphthalen-1-amine (24)**. Green oil. Yield: 30%. Found: C, 67.03; H, 4.64; N, 8.73. $C_{27}H_{22}BrN_3O$ requires C, 66.95; H, 4.58; N, 8.67. ν_{max}/cm^{-1} 3049, 2859, 2359, 1894, 1732, 1581, 1289, 770, 420. ^{1}H NMR δ_H (300 MHz; DMSO-d$_6$) 8.02 (d, *J* = 6.9 Hz, 1 H), 7.73 (d, *J* = 7.1 Hz, 1 H), 7.57 (d, *J* = 8.5 Hz, 2 H), 7.54-7.40 (m, 4 H), 7.20-7.09 (m, 3 H), 7.08-7.00 (m, 4 H), 6.31-6.29 (m, 2 H), 4.31-4.29 (m, 2 H),

3.41-3.39 (m, 2 H). ^{13}C NMR δ_C (75 MHz; DMSO-d_6) 156.0, 155.7, 143.2, 139.0, 134.1, 133.0, 131.5, 130.5, 128.0, 127.4, 126.7, 125.7, 125.3, 124.1, 123.1, 121.5, 121.0, 118.8, 116.0, 115.5, 103.0, 43.8, 43.1. m/z 485 (M^+)

2,4-Difluoro-3-(1-(2-(naphthalen-1-ylamino)ethyl)-1H-imidazol-5-yl)phenol (25). Brown solid. Yield: 35%. mp 190-191 °C. Found: C, 69.18; H, 4.73; N, 11.57. $C_{21}H_{17}F_2N_3O$ requires C, 69.03; H, 4.69; N, 11.50. ν_{max}/cm^{-1} 3371, 2866, 2359, 1732, 1582, 1470, 1252, 1109, 1092, 879, 404. ^{1}H NMR δ_H (300 MHz; DMSO-d_6) 8.03 (d, *J* = 7.9 Hz, 1 H), 8.00 (s, 1 H), 7.73 (d, *J* = 7.7 Hz, 1 H), 7-45-7.36 (m, 2 H), 7.17-6.98 (m, 5 H), 6.30 (br t, *J* = 5.2 Hz, 1 H), 6.17 (d, *J* = 6.9 Hz, 1 H), 4.12 (t, *J* = 6.6 Hz, 2 H), 3.40 (m, 2 H). ^{13}C NMR δ_C (75 MHz; DMSO-d_6) 152.8 (d, *J* = 232.4 Hz), 149.2 (d, *J* = 229.3), 143.6, 142.4 (d, *J* = 12.0 Hz), 140.0, 134.5, 130.2, 128.6, 127.1, 126.3, 124.7, 123.5, 121.9, 119.7, 118.8 (m), 116.7, 111.6 (d, *J* = 27.0 Hz), 107.4 (dd, *J* = 12.0, 11.5 Hz), 103.0, 44.2, 43.7. m/z 366 (M^+)

2,4-Dibromo-6-(1-(2-(naphthalen-1-ylamino)ethyl)-1H-imidazol-5-yl)phenol (26). Green solid. Yield: 47%. mp 130-131 °C. Found: C, 51.79; H, 3.58; N,8.62. $C_{21}H_{17}Br_2N_3O$ requires C, 51.77; H, 3.52; N, 8.63. ν_{max}/cm^{-1} 3440, 3066, 2921, 1739, 1584, 1225, 1109, 768. ^{1}H NMR δ_H (300 MHz; DMSO-d_6) 7.87-7.72 (m, 3 H), 7.97 (m, 1H), 7.42-7.32 (m, 3 H), 7.18-7.07 (m, 2 H), 6.94 (s, 1 H), 6.15 (d, *J* = 7.4 Hz, 1 H), 4.48 (br s, 1 H), 4.11 (t, *J* = 6.3 Hz, 2 H), 3.36 (m, 2 H). ^{13}C NMR δ_C (75 MHz; DMSO-d_6) 152. 5, 143.7, 135.5, 134.6, 134.2, 133.6, 129.5, 128.8, 127.2, 126.2, 124.7, 123.5, 122.0, 117.8, 116.5, 115.3, 113.5, 111.4, 103.1, 42.3, 42.1. m/z 488 (M^+)

3-Chloro-4-(1-(2-(naphthalen-1-ylamino)ethyl)-1H-imidazol-5-yl)phenol (27). Green solid. Yield: 55%. mp 103-104 °C. Found: C, 69.37; H, 5.02; N, 11.60. $C_{21}H_{18}ClN_3O$ requires C, 69.32; H, 4.99; N, 11.55. ν_{max}/cm^{-1} 2755, 2561, 1728, 1581, 1439, 1286, 1109, 770. ^{1}H NMR δ_H (300 MHz; DMSO-d_6) 8.03 (d, *J* = 7.1 Hz, 1 H), 7.86 (s, 1 H), 7.72 (d, *J* = 6.9 Hz, 1 H), 7.44-7.35 (m, 2 H), 7.24 (d, *J* = 8.2 Hz, 1 H), 7.13-7.07 (m, 2 H), 7.00 (d, *J* = 2.2 Hz, 1H), 6.88 (s, 1 H), 6.82 (dd, *J* = 8.2, 2.2 Hz, 1 H), 6.31 (t, *J* = 5.5 Hz, 1 H), 6.01 (dd, *J* = 6.3, 2.5 Hz, 1 H), 4.04 (m, 2 H), 3.34 (m, 2 H). ^{13}C NMR δ_C (75 MHz; DMSO-d_6) 164.0, 148.0, 143.0, 139.5, 139.0, 138.9, 133.9, 133.0, 132.9, 131.4, 130.5, 129.0, 127.9, 126.3, 123.7, 121.0, 120.7, 119.5, 107.3, 48.5, 45.2. m/z 364 (M^+)

2-(1-Cyclopropyl-1H-imidazol-5-yl)-4-methoxyphenol (28). Orange solid. Yield: 36%. mp 204-205 °C. Found: C, 67.85; H, 6.21; N, 12.17. $C_{13}H_{14}N_2O_2$ requires C, 67.81; H, 6.13; N, 12.17. ν_{max}/cm^{-1} 2828, 1814, 1600, 1513, 1279, 1214, 1113, 937. ^{1}H NMR δ_H (300 MHz; $CDCl_3$) 7.63 (s, 1 H), 7.01 (s, 1 H), 6.96 (d, *J* = 8.8 Hz, 1 H), 6.87 (d, *J* = 8.8 Hz, 1 H), 6.77 (s, 1 H), 3.77 (s, 3 H), 3.31 (m, 1 H), 0.86-0.81 (m, 4 H). ^{13}C NMR δ_C (75 MHz; DMSO-d_6) 152.3, 149.7, 138.1, 131.6, 128.3, 118.3, 116.8, 116.6, 115.5, 55.9, 27.4, 6.7. m/z 231 (M^+)

***N*-(2-(5-(4-phenoxyphenyl)-1H-imidazol-1-yl)ethyl)acetamide (29).** Yellow oil. Yield: 26%. Found: C, 71.00; H, 5.98; N, 13.10. $C_{19}H_{19}N_3O_2$ requires C, 71.01; H, 5.96; N, 13.08. ν_{max}/cm^{-1} 3064, 2031, 1658, 1488, 1231, 756. ^{1}H NMR δ_H (300 MHz; CD_3OD) 7.74 (s, 1 H), 7.40-7.32 (m, 4 H), 7.13 (t, *J* = 7.4 Hz, 1 H), 7.09-6.97 (m, 4 H), 6.96 (s, 1 H), 4.15 (t, *J* = 6.0 Hz, 2 H), 3.30 (t, *J* = 6.0 Hz, 2 H), 1.79 (s, 3 H). ^{13}C NMR δ_C (75 MHz; DMSO-d_6) 170.2, 157.0, 156.8, 139.3, 131.7, 130.8, 130.7, 128.0, 125.4, 124.4, 119.6, 119.1, 55.4, 42.6, 22.9. m/z 322 (M^+)

4-Methoxy-2-(1-propyl)-1H-imidazol-5-yl)phenol (30). Yellow solid. Yield: 50%. Found: C, 67.29; H, 6.99; N, 12.05. $C_{13}H_{16}N_2O_2$ requires C, 67.22; H, 6.94; N, 12.06. ν_{max}/cm^{-1} 3143, 2964, 1807, 1556, 1497, 1449, 1209, 801. ^{1}H NMR δ_H (300 MHz; DMSO-d_6) 7.70 (s, 1 H), 6.87-6.70 (m, 3 H), 6.68 (s, 1 H), 3.84 (t, *J* = 7.1 Hz, 2 H), 3.68 (s, 3 H), 1.19 (sex, *J* = 7.4 Hz, 2 H), 0.68 (t, *J* = 7.4 Hz, 3 H). ^{13}C NMR δ_C (75 MHz; DMSO-d_6) 152.1, 149.1, 137.9, 129.9, 127.6, 117.8, 116.7, 116.5, 115.3, 55.5, 46.7, 23.6, 11.0. m/z 233 (M^+)

Biology

Cell culture. Human A375 cells were cultured in DMEM medium with high glucose (4.5 g/L), containing 10% heat inactivated fetal bovine serum (FBS), 2 mM L-glutamine 100 U/mL of penicilline and 10 µ/mL of streptomycine (GE Healthcare, Milan, Italy). Cells were cultured in a humidified atmosphere (5% CO_2, 37 °C).

Cell cytotoxicity. Cell viability was measured by the 3-(4,5-dimethylthiazol-2-yl)-2,5-diphenyl-tetrazolium bromide (MTT) assay, as previously described.[25] A375 cells were seeded (0.5 x 10^5 cells/well) in 24-well plates and treated with increasing concentrations (0.01–100 µM) of each compound for 48 h at 37 °C in a 5% CO_2 humidified incubator. The percentage of cell viability was calculated as [100 (x−y)/ (z−y)], where x, y, and z were the absorbance read in compound-treated, resting and compound untreated cells, respectively.

Cellular IDO1 enzymatic assay. The enzymatic activity of IDO1 was evaluated by measuring the levels of L-KYN into A375 cell media, as previously described.[26] A375 cells (5X10^4) were seeded in a 24-well culture plate (500 µL/well) and grown overnight. Serial DMSO dilutions (0.01–30 µM) of each compounds in a total volume of 500 µL culture medium including a 100 µM L-tryptophan (Sigma-Aldrich) and human IFN-γ (500 U/mL final concentration) per well were added into wells containing the cells. All compounds were dissolved in DMSO (Sigma–Aldrich). The DMSO final concentration in cell culture medium was always 0.1%. Equivalent amount of DMSO was always added to drug untreated controls. After 48h incubation, cell medium was collected, deproteinized by 20% (v/v) aqueous CCl_3COOH, centrifuged at 13,200 rpm for 10 minutes, and the amounts of L-KYN in A375 cell media were quantified with HPLC. 20 µL of supernatants were injected by a multi-sampler (Beckman Coulter, Milan, Italy) into a HPLC-UV-VIS system (System Gold Beckman Coulter), equipped with a C-18 sphereClone ODS analytical column (5 µm particle size, 250 mm x 4.0 mm; Phenomenex, Torrance, CA, USA). The mobile phase (50 mM potassium dihydrogen phosphate, 10% v/v acetonitrile; pH 4.8) was delivered at a flow-rate of 1 mL/min at room temperature, and the absorbance was measured at 330 nm. Amounts of L-KYN in A375 cell media were quantified on the basis of a calibration curve obtained using the same HPLC-UV-VIS experimental setting.
IC_{50} values were calculated from concentration-response curves obtained in at least three different experiments run in triplicate.

rhIDO1 enzymatic assay. rhIDO1 activity was determined as follows. In brief, the standard reaction mixture (200 µL) contained 50 mM potassium phosphate buffer (KPB) (pH 6.5), 20 mM ascorbic acid (neutralized with NaOH and HCl) (Sigma Aldrich), 100 µg/mL catalase (Sigma Aldrich), 10 µM methylene blue (Alfa Aesar),

Heysham, Lancashire, United Kingdom), 100 µM L-tryptophan (Sigma Aldrich), 50 nM rhIDO1 (Origene, Bologna, Italy), and dimethyl sulfoxide (DMSO) solution of the compound (4 µL). The reaction was carried out at 37 °C for 60 min and stopped by the addition of 40 µL of 30% (w/v) CCl_3COOH. After heating at 50 °C for 15 min, the reaction mixture was centrifuged at 1500 g for 10 min. The supernatant (150 µL) was transferred into a well of a 96-well microplate and mixed with 150 µL of 2% (w/v) *p*-dimethylaminobenzaldehyde (Ehrlich's reagent) in acetic acid. The yellow pigment derived from kynurenine was measured at 490 nm using an Ultramark Microplate Imaging System (Bio-Rad). IC_{50} values were calculated from concentration-response curves obtained in at least three different experiments run in triplicate.

Statistical analysis. Results are expressed as means ± SEM of at least three different experiments run in triplicate. The software GraphPad 5.0 for Windows (GraphPad Software, La Jolla, California, USA) was used as a nonlinear regression model for analysis of the concentration–response data to obtain the 50% inhibitory concentration value (IC_{50}).

Molecular modeling

All molecular modeling studies were performed on a Tesla workstation equipped with two Intel Xeon X5650 2.67 GHz processors and Ubuntu 10.04 (www.ubuntu.com). Different software was used to elaborate the chemical information: PerlMol[27] and OpenEye (www.eyesopen.com) applications. The protein structures and 3D chemical structures were generated in PyMol.[24]

Compounds source. The collection of reactants was retrieved from ZINC.[28] This searchable database includes chemical structures available from chemical vendors. The structures were downloaded using the web-based interface and filtered using FILTER software[29] from OpenEye to select compounds containing aldehyde, amine or TosMIC moieties. Additionally, we made 300 Daltons the upper limit for the molecular weights for the structures, facilitating compatibility with synthetic drugs. Using these criteria, 932 aldehydes, 983 amines and 54 TosMIC were retrieved. The reactants were saved as canonical SMILES.

Generation of database. An *in house* perl script based on PerlMol[27] was used to retrieve each reactant and perform a virtual combinatorial reaction with all downloaded compounds. The resulting structures were filtered using Lipinski's rule of 5,[30] the most stable tautomers were calculated and the retained SMILES for 1,4,5-trisubstituted (49,472,424 compounds), 1,5-disubstituted (916,156 compounds), 1,4-disubstituted (53,082 compounds) and 4,5-disubstituted (50,328 compounds) imidazoles were saved. Each structure was rebuilt as a 3D structure using OMEGA2.[18]

Preparation of protein. The X-ray structure of the 4-phenylimidazole-IDO1 complex was used in this study, entry code 2D0T.[6] Water molecules were removed, all hydrogen atoms and MMFF94 charges were added. Then, the complex was transferred into fred_receptor and prepared for docking with FRED.[19] The interaction with iron moiety of heme group was used as a constraint: if an atom of the molecule was within an acceptable distance to it, the docking pose was retained; if not, the compound was discarded.

Virtual screening procedure. Conformations were generated for all structures using OMEGA2 (maximum number of conformations: 350, rmsd threshold: 1.0 Å),[18] and charges were assigned according to MMFF94 scheme.[31] Docking was performed with FRED.[19] Docked conformations were scored using Chemgauss4 (see Supporting Information for the docked pose of the synthesized compounds).[32]

3D-QSAR conformer generation. 4-PI (**1**) and 4,5-disubstituted imidazoles **6**-**20** were taken into account. The sixteen compounds used to generate the 3D-QSAR model were processed using OpenEye software suite according to the following scheme: FixPKA[33] to assign correct protonation at pH 7, tautomers in order to generate the most aromatic tautomer for each compound and finally OMEGA2[18] to generate one minimized 3D conformation for each compound in sdf file format. As we wanted to focus on 4,5-diarylimidazoles, the inactive compound **14,** that displays a benzyl substituent, was removed from the list of molecules used to build the 3D-QSAR model.

3D-QSAR model generation. According to the Open3DTools[27] workflow the sdf containing all data set was processed with Open3DAlign,[22] which generates one structure-and-field based alignment of the data set using each compound in the file as a template and leading to fifteen different alignments. Following visual inspection, the alignment 0012 based on compound **13** was selected to perform the analysis, taking into account alignment scores and superposition of imidazole substituents. In particular, in this alignment the smaller substituents were all identically oriented as well as the more hindered ones (See Supplementary Information for a pocket-binding hypothesis of compounds **1** and **6**-**20**). IC_{50} values were converted to pIC_{50} and added to the sdf file. In this step we set to an arbitrary value (150 µM) the IC_{50} for compounds **1** and **13**, while the IC_{50} values of **12** and **19** were extrapolated as these compounds inhibited IDO activity without reaching the maximal inhibition at the highest concentration tested (30 µM). The data set was split into a training set and a test set (containing respectively 75% and 25% of the total compounds). In order to generate a consistent statistical model we selected the compounds of the training and test sets so that they span across the entire range of pIC_{50} values (see Supplementary Information). The analysis was performed with Open3DQSAR software and then the model was evaluated again using command line version of Forge[23] skipping in software alignment and conformational hunt, and using LOO type cross validation (R^2 = 0.998, Q^2 = 0.555) (see Supplementary Information).

Conclusions

4-PI is a non-competitive inhibitor of IDO1 and represents a promising starting point for the development of more potent compounds, as demonstrated by the amount of patents displaying imidazoles as IDO1 inhibitors and by the recent introduction of the fused imidazole NLG919 into Phase

clinical trials. The van Leusen multicomponent reaction has the potential to generate large and diverse libraries of imidazoles: thus, in order to reduce the number of theoretical possibilities to a practical level for synthesis and testing, a virtual screening approach was used and afforded a series of 4,5- and 1,5-disubstituted imidazoles as putative IDO1 inhibitors. These compounds were synthesized and tested, leading to the identification of four 4,5-disubstituted imidazoles that display a 10-fold improvement in potency compared to 4-PI in enzymatic assay, are able to permeate the cell membrane, in contrast to **1**, and show no detectable toxicity in cells. A 3D-QSAR analysis applicable to 4,5-diaryl imidazoles was performed. A putative hydrogen bond between the NH of the imidazole ring and Ser167 of the protein might be responsible for the improvement of potency, together with favorable interactions with the partially occupied pocket B.

The information obtained in this study, together with the performed 3D-QSAR analysis, demonstrate that the 4,5-disubstituted imidazole scaffold might provide a new direction for future design of IDO1 inhibitors. Further efforts to discover promising candidates are in progress and aim to optimize molecular recognition by pocket B: this would help to increase potency together with selectivity for IDO1 over other targets and especially heme proteins.

Acknowledgements

This study was financially supported by Associazione Italiana per la Ricerca sul Cancro (AIRC) (Grant 15918), Italy. We also gratefully acknowledge support from Ministero dell'Istruzione, dell'Università e della Ricerca (MIUR) (PRIN 2010-2011; Grant 2010W7YRLZ_002), Italy.

Notes and references

1 D. H. Munn and A. L. Mellor, *Trends Immunol.* 2013, **34**, 137-143.
2 M. Platten, W. Wick and B. J. Van den Eynde, *Cancer Res.* 2012, **72**, 5435-5440; G. C. Prendergast, C. Smith, S. Thomas, L. Mandik-Nayak, L. Laury-Kleintop, R. Metz and A. J. Muller, *Cancer Immunol. Immunother.* 2014, **63**, 721-735; J. M. Gostner, K. Becker, F. Uberall and D. Fuchs, *Expert Opin. Ther. Targets* 2015, **19**, 605-615.
3 J. Godin-Ethier, L.-A. Hanafi, C. A. Piccirillo and R. Lapointe, *Clin. Cancer Res.* 2011, **17**, 6985-6991.
4 E. Dolusic and R. Frederick, *Expert Opin. Ther. Patents* 2013, **23**, 1367-1381; U. F. Rohrig, S. R. Majjigapu, P. Vogel, V. Zoete and O. Michielin, *J. Med. Chem.* 2015, DOI: 10.1021/acs.jmedchem.5b00326.
5 B. Baban, P. Chandler, D. McCool, B. Marshall, D. H. Munn and A. L. Mellor, *Curr. Cancer Drug Targets* 2009, **9**, 938-952.
6 H. Sugimoto, S. Oda, T. Otsuki, T. Hino, T. Yoshida and Y. Shiro, *Proc. Natl. Acad. Sci. USA* 2006, **103**, 2611-2616.
7 M. Sono and S. G. Cady, *Biochemistry* 1989, **28**, 5392-5399.
8 S. Kumar, D. Jaller, B. Patel, J. M. LaLonde, J. B. DuHadaway, W. P. Malachowski, G. C. Prendergast and A. J. Muller, *J. Med. Chem.* 2008, **51**, 4968-4977.
9 WO2009132238, 2009.
10 WO2011056652, 2011.
11 WO2012142237, 2012.
12 NCT02048709, https://clinical trials.gov, (accessed July 2015); S. Crunkhorn, *Nat. Rev. Drug Dis.* 2014, **13**, 879.
13 S. Tojo, T. Kohno, T. Tanaka, S. Kamioka, Y. Ota, T. Ishii, K. Kamimoto, S. Asano and Y. Isobe, *ACS Med. Chem. Lett.* 2014, **5**, 1119-1123.
14 Dömling A, W. Wang and K. Wang, *Chem. Rev.* 2012, **112**, 3083-3135.
15 M. Guasconi, X. Lu, A. Massarotti, A. Caldarelli, E. Ciraolo, G. C. Tron, E. Hirsch, G. Sorba and T. Pirali, *Org. Biomol. Chem.* 2011, **9**, 4144-4149; T. Pirali, V. Faccio, R. Mossetti, A. A. Grolla, S. Di Micco, G. Bifulco, A. A. Genazzani and G. C. Tron, *Mol. Div.* 2010, **14**, 109-121; A. A. Grolla, V. Podestà, M. G. Chini, S. Di Micco, A. Vallario, A. A. Genazzani, P. L. Canonico, G. Bifulco, G. C. Tron, G. Sorba and T. Pirali, *J. Med. Chem.* 2009, **52**, 2776-2785.
16 A. M. van Leusen, J. Wildeman and O. H. Oldenziel, *J. Org. Chem.* 1977, **42**, 1153-1159; J. Sisko, A. J. Kassick, M. Mellinger, J. J. Fiulan, A. Allen and M. A. Olsen, *J. Org. Chem.* 2000, **65**, 1516-1524; D. van Leusen and A. M. van Leusen, In *Organic Reactions*, Overman, L. E., Ed.; John Wiley & Sons: New York, 2001, vol. 57. pp. 417.
17 J. Sisko and M. Mellinger, *Pure Appl. Chem.* 2002, **74**, 1349.
18 OMEGA, version 2.4.6; OpenEye Scientific Software: Santa Fe, NM. http://www.eyesopen.com; P. C. D Hawkins, A. Skillman, G. L. Warren, B. A. Ellingson and M. T. Stahl, *J. Chem. Inf. Model.* 2010, **50**, 572−584; P. C. D. Hawkins and A. Nicholls, *J. Chem. Inf. Model.* 2012, **52**, 2919-2936.
19 FRED, version 3.0.0; OpenEye Scientific Software: Santa Fe, NM. http://www.eyesopen.com; McGann, M. *J. Chem. Inf. Model.* 2011, **51**, 578−596.
20 J. Sisko, M. Mellinger, P. W. Sheldrake P. W. and N. H. Baine, *Tetrahedron Lett.* 1996, **37**, 8113-8116; J. Sisko, M. Mellinger, P. W. Sheldrake and N. H. Baine, *Org. Synth.* 2000, **77**, 198-202.
21 J. Sisko, A. J. Kassick, M. Mellinger, J. J. Fiulan, A. Allen and M. A. Olsen, *J. Org. Chem.* 2000, **65**, 1516-1524.
22 P. Tosco, T. Balle and F. Shiri *J. Comput. Aided Mol. Des.* 2011, **25**, 777-783.
23 Cresset Group. http://www.cresset-group.com/products/forge/. Forge V.10
24 The PyMOL Molecular Graphics System, version 1.3; Schrödinger LLC: 2010.
25 S. Fallarini , T. Paoletti, C. O. Battaglini, P. Ronchi, L. Lay, R. Bonomi, S. Jha, F. Mancin, P. Scrimin and G. Lombardi, *Nanoscale* 2013, **5**, 390-400.
26 S. Fallarini, T. Paoletti, L. Panza and G. Lombardi, *Biochem. Pharmacol.* 2008, **76**, 738-750.
27 I. Tubert-Brohman, *Perl J.* 2004, **8**, 3-5; I. Tubert-Brohman 2004. http://www.perlmol.org.
28 J. J. Irwin, T. Sterling, M. M. Mysinger, E. S. Bolstad and R. G. Coleman, *J. Chem. Inf. Model.* 2012, **52**, 1757−1768.
29 FILTER, version 2.0.2; OpenEye Scientific Software: Santa Fe, NM. http://www.eyesopen.com.
30 J. Lipinski, *Pharmacol. Toxicol. Methods* 2000, **44**, 235-49.
31 T. A. Halgren, *J. Comput. Chem.* 1996, **17**, 520-552.
32 M. R. McGann, H. R. Almond, A. Nicholls, J. A. Grant and F. K. Brown, *Biopolymers* 2003, **68**, 76-90.
33 Quacpac, version 1.6.3.1; OpenEye Scientific Software: Santa Fe, NM. http://www.eyesopen.com.

A virtual library of 50,000,000 compounds synthesizable via the van Leusen MCR was created, screened and filtered to afford a series of disubstituted imidazoles with improved properties compared to the parent compound 4-phenylimidazole.

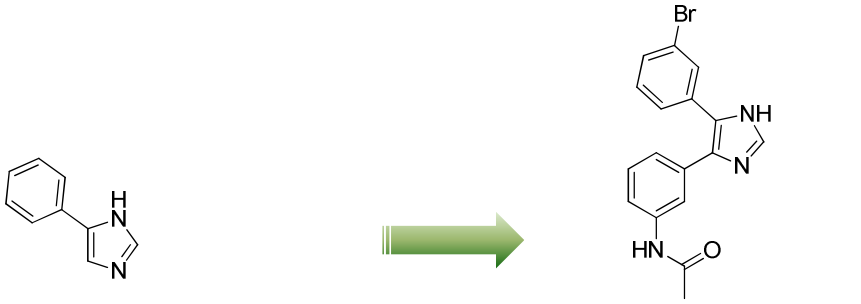

1
IC_{50} (rhIDO) = 48.0 µM
IC_{50} (A375) > 30 µM

15
IC_{50} (rhIDO) = 2.8 µM
IC_{50} (A375) = 2.9 µM